Research article

Chunyang Ma, Weichun Huang, Yunzheng Wang, Jordan Adams, Zhenhong Wang, Jun Liu, Yufeng Song, Yanqi Ge, Zhongyi Guo, Lanping Hu and Han Zhang*

MXene saturable absorber enabled hybrid mode-locking technology: a new routine of advancing femtosecond fiber lasers performance

https://doi.org/10.1515/nanoph-2019-0527
Received December 17, 2019; revised March 3, 2020; accepted March 14, 2020

Abstract: MXene is a promising two-dimensional (2D) material that is widely used in electro-photonic devices due to its unique properties. In this contribution, V_2CT_x, a novel MXene, was employed as a saturable absorber (SA) for hybrid passively mode-locked fiber lasers. An ultra-stable and self-starting mode-locked laser system with low threshold can be achieved using V_2CT_x nanosheets and nonlinear polarization evolution (NPE). Signal to noise ratio increased 13 dB compared with using only NPE SA. A 72 fs pulse duration is easily achieved from this hybrid mode-locked fiber laser system. To the best of our knowledge, this is the shortest pulse duration generated from the Yb-doped mode-locked fiber lasers using a hybrid or 2D SAs. This study proves that MXene V_2CT_x nanosheets can be developed as suitable SAs and served as potential advanced ultrafast photonic devices in the future.

Keywords: MXene; V_2CT_x; layered materials; nonlinear photonics; ultrafast fiber lasers.

1 Introduction

Ultrafast fiber lasers have become more attractive in recent years due to the advantages of compactness, low-cost, high beam quality, efficient heat dissipation, etc. Ultra-short pulses with high energy are suitable for certain cutting-edge applications such as ophthalmology [1], high-order harmonic generation [2], bio imaging [3], nonlinear microscopy [4], frequency comb [5, 6], and nanofabrication [7]. Fast saturable absorbers (SAs) which

***Corresponding author: Han Zhang,** Institute of Microscale Optoelectronics, Collaborative Innovation Centre for Optoelectronic Science and Technology, International Collaborative Laboratory of 2D Materials for Optoelectronics Science and Technology of Ministry of Education, Key Laboratory of Optoelectronic Devices and Systems of Ministry of Education and Guangdong Province, College of Physics and Optoelectronic Engineering, Shenzhen Key Laboratory of Micro-Nano Photonic Information Technology, Guangdong Laboratory of Artificial Intelligence and Digital Economy (SZ), Shenzhen University, Shenzhen 518060, PR China, e-mail: hzhang@szu.edu.cn. https://orcid.org/0000-0002-9131-9767
Chunyang Ma, Yunzheng Wang, Zhenhong Wang, Jun Liu, Yufeng Song and Yanqi Ge: Institute of Microscale Optoelectronics, Collaborative Innovation Centre for Optoelectronic Science and Technology, International Collaborative Laboratory of 2D Materials for Optoelectronics Science and Technology of Ministry of Education, Key Laboratory of Optoelectronic Devices and Systems of Ministry of Education and Guangdong Province, College of Physics and Optoelectronic Engineering, Shenzhen Key Laboratory of Micro-Nano Photonic Information Technology, Guangdong Laboratory of Artificial Intelligence and Digital Economy (SZ), Shenzhen University, Shenzhen 518060, PR China. https://orcid.org/0000-0002-6478-628X (Y. Song)
Weichun Huang: Institute of Microscale Optoelectronics, Collaborative Innovation Centre for Optoelectronic Science and Technology, International Collaborative Laboratory of 2D Materials for Optoelectronics Science and Technology of Ministry of Education, Key Laboratory of Optoelectronic Devices and Systems of Ministry of Education and Guangdong Province, College of Physics and Optoelectronic Engineering, Shenzhen Key Laboratory of Micro-Nano Photonic Information Technology, Guangdong Laboratory of Artificial Intelligence and Digital Economy (SZ), Shenzhen University, Shenzhen 518060, PR China; and Nantong Key Lab of Intelligent and New Energy Materials, College of Chemistry and Chemical Engineering, Nantong University, Nantong 226019, Jiangsu, PR China. https://orcid.org/0000-0002-1948-8347
Jordan Adams: Department of Electro-Optics and Photonics, University of Dayton, Dayton, OH 45469, USA
Zhongyi Guo: School of Electrical Engineering and Intelligentization, Dongguan University of Technology, Dongguan 523808, PR China
Lanping Hu: Nantong Key Lab of Intelligent and New Energy Materials, College of Chemistry and Chemical Engineering, Nantong University, Nantong 226019, Jiangsu, PR China

possess high modulation depth with nearly instantaneous response time are always desirable to generate ultra-short pulses, especially in the all-normal dispersion regime where the mode-locking mechanism is not dominated by soliton-like pulse shaping. Nonlinear polarization evolution (NPE) is the most common SA used in femtosecond dissipative soliton and similariton fiber lasers [8–12]. However, mode-locking with a fast SA has the unavoidable self-starting difficulty; continuous wave to mode-locked operation requires initiation methods because of an insufficient pulse shaping effect for long pulse [13]. Interestingly, it is pointed out that a self-starting mode-locked operation can be easily initiated and stabilized by the saturation dynamics of slow SAs but struggle to generate ultra-short pulses. Their slow recovery causes trailing wings to develop requiring additional soliton-like pulse shaping to achieve femtosecond pulses [14].

Alternatively, a new mode-locked function, called hybrid mode-locking has been studied extensively. This uses a fast and slow SA together permitting a self-starting laser system with ultra-short pulse generation. The fast SA response shapes the pulse into durations reaching the femtosecond regime while the slow SA facilitates pulse initiation process and stabilizes the mode-locked operation [14–16].

A slow SA with a suitable saturation dynamic is crucial for hybrid mode-locked fiber lasers. In recent years, a wide range of two-dimensional (2D) materials have been used in optoelectronic and nonlinear photonic applications due to its unique properties [17–20] with significant use as slow SAs in passively mode-locked (PML) fiber lasers, which tend to be a potential candidate as the excellent slow SAs [21–23]. In 2009, graphene was successfully used in PML fiber lasers [24, 25], but the inherent zero bandgap structure and low modulation depth (usually <1%) limit laser output performance and practical applications. Also because of extensive research, it has been found that black phosphorus and bismuth (Bi) can be easily peeled off from its bulk crystal by mechanical exfoliation or liquid phase exfoliation [26, 27], but chemical instability to atmospheric humidity makes them difficult to be applied [28, 29]. Transition metal dichalcogenides (TMDs) display strong bulk-like photon absorption and exciton generation and have been used in lasers, but only single-layer MX_2 exhibits direct band gap properties, largely hindering applications [30]. In contrast to these, a new 2D material called MXene has potential benefits for ultrafast photonics. The general chemical formula of MXene materials is $M_{n+1}X_nT_x$ ($n = 1, 2, 3$), where M is a transition metal (Sc, Ti, Zr, V, Nb, Cr, or Mo), X represents C or N, T is an element from the third or fourth main group (-OH, -O, or -F), and x refers to the number of terminal groups. The popular MXene compound $Ti_3C_2T_x$ has already been used in electro-optic devices with advantages due to its narrow band gap and high photothermal effect [31–34]. However, in open vials $Ti_3C_2T_x$ MXene solutions degrade into cloudy-white colloidal solutions containing primarily anatase (TiO_2) [35], making it impractical for many applications. Therefore, it is necessary to develop new kind of MXenes with high performance for the hybrid mode-locked fiber lasers.

In this article, we demonstrate the successful synthesis of MXene V_2CT_x nanosheets by HF selective etching method followed by the delamination of as-etched V_2C. The MXene together with NPE creates a hybrid mode-locker that generates 72 fs pulses from Yb-doped fiber laser. To the best of our knowledge, this is the shortest pulse duration in the field of hybrid mode-locking. In contrast to NPE alone, the hybrid structure of MXene and NPE can realize self-starting in addition to a signal to noise ratio (SNR) increase of 13 dB of ultra-short pulses. This proves that hybrid mode-locking is a new routine for advancing femtosecond fiber laser performance.

2 Fabrication and characterization of MXene (V_2CT_x)

To prepare the V_2C powder, 2.0 g V_2AlC (200 mesh) was added into 40 ml HF (30%) under continuous stirring at 35°C for 48 h. After the reaction, the mixture was diluted by deionized water (DI H_2O), and then centrifuged for a couple of times (5000 rpm, 10 min per cycle) until the pH of the supernatant was more than 6. The etched V_2AlC was collected by filtration using PVDF membrane (0.45 μm mesh) and washed with a large quantity of DI H_2O (~2L). Similar to the delamination protocol for Ti_3C_2 powder, the etched V_2AlC slurry was first dispersed into DI H_2O, followed by being delaminated in a sonication bath with a built-in water-cooling system for 30 min at 400 W. The temperature was fixed at 10°C throughout the sonication process. Afterwards, the dispersion was initially centrifuged at a speed of 5000 rpm for 30 min giving a supernatant containing V_2CT_x nanosheets. This was gently decanted to another test tube and further centrifuged at a centrifugation speed of 18,000 rpm for another 30 min. The obtained precipitate was dried at 80°C under vacuum overnight.

Figure 1 gives the structural characterization of the etched V_2AlC and exfoliated V_2CT_x nanosheets. The basal planes fan out and spread apart after HF treatment (Figure 1A), suggesting the successful removal of Al in V_2AlC. Transmission electron microscopy (TEM)

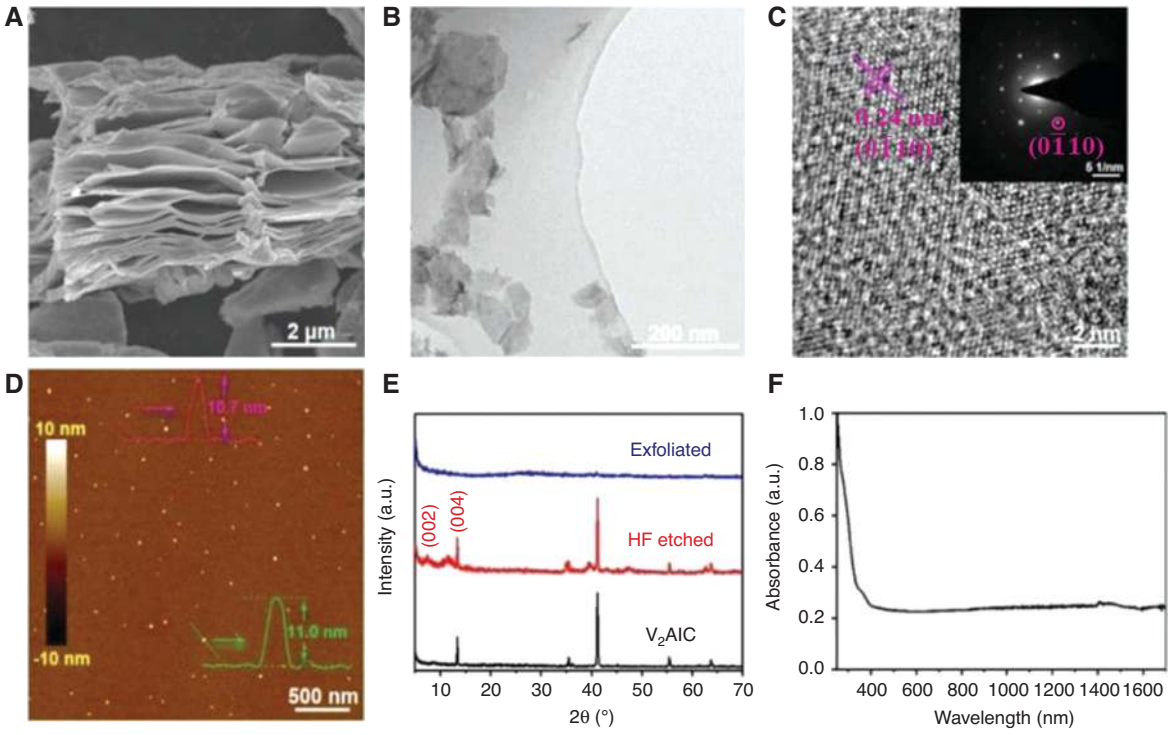

Figure 1: The structural characterization of MXene (V_2CT_x).
(A) Scanning electron microscopic image of MAX after selective removal of Al. (B) Transmission electron microscopic (TEM) image of exfoliated V_2CT_x nanosheets. (C) High-resolution TEM of exfoliated V_2CT_x nanosheets. (D) Atomic force microscopic image of exfoliated V_2CT_x nanosheets. (E) X-ray diffraction of V_2AlC, etched V_2AlC, and exfoliated V_2CT_x nanosheets. (F) Ultraviolet-visible-near infrared spectroscopy of exfoliated V_2CT_x nanosheets.

analysis of exfoliated nanosheets (Figure 1B) exhibits the as-prepared V_2CT_x nanosheets to be quite thin with ~50 to ~200 nm lateral range. The crystal structure was further confirmed by high-resolution TEM and selected area electron diffraction, exhibiting a set of clear lattice fringes with an inner plane spacing of 0.24 nm (Figure 1C), corresponding to the (0$\bar{1}$10) plane of MXene V_2C, Figure 1C, in good agreement with previous results [36, 37]. Atomic force microscopy was employed to further investigate the as-synthesized MXene V_2CT_x nanosheets (Figure 1D). The thicknesses of the as-synthesized MXene V_2CT_x nanosheets are measured to ~11 nm, which correspond to around 11 layers of MXene V_2C [37, 38]. The X-ray powder diffraction (XRD) patterns of V_2AlC, V_2C, and V_2CT_x nanosheets (Figure 1E) indicate that the (002) peak at 8.6° in the XRD pattern of V_2C appears after the Al-layer in V_2AlC has been selectively etched in a HF solution, suggesting the successful selective etching of V_2AlC. Besides, no obvious XRD signal can be observed after exfoliation, implying that the as-etched V_2C has been sufficiently exfoliated. Figure 1F shows the absorption result of the as-synthesized V_2CT_x nanosheets, exhibiting absorption range from 280 to 2000 nm, implying the broad bandwidth operation range of the material. Moreover, Tauc plot (Figure S1) of the as-synthesized V_2CT_x nanosheets was obtained based on the absorption data with narrow bandgap of 0.43 eV.

3 Nonlinear optical responses of MXene (V_2CT_x)

The SA was fabricated by depositing V_2CT_x nanosheets on tapered fiber. The tapered fiber was home-made by the fiber-tapering equipment with HI-1060 fiber. The length of the fiber taper was about 3 mm with a waist diameter of ~5.2 μm. The diagram of the optical deposition method is shown in Figure 2A. A 980-nm pump laser was used in the fabrication process and the power meter monitored the power change in real time. V_2CT_x nanosheets were dropped on the microfiber with a pipette; the V_2CT_x was adsorbed on the surface of the microfiber due to the evanescent field action. Real-time observation of the loss of the fiber facilitates was used to control the depth of deposition which took about 10 min. Figure 2B shows the optical microscope image of the microfiber deposited with V_2CT_x MXene.

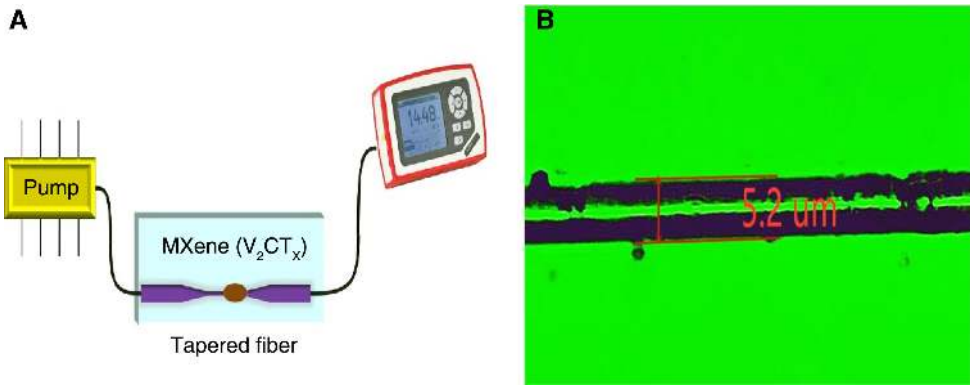

Figure 2: Experiment of V_2CT_x deposition on tapered fiber.
(A) Diagram of the optical deposition method. (B) Optical microscopic image.

The absorption measurement of the MXene-based SA was carried out using a balanced twin-detector (Figure 3A). A femtosecond pulsed fiber laser centered at 1064 nm with a 30 MHz repetition rate was used as the pump light source. After the laser passed through an adjustable attenuator, its output was split by a 50:50 fiber coupler where one beam was used as a reference signal (detector 1) and the other for detecting the nonlinear absorption of V_2CT_x (detector 2).

The transmitted power versus incident power was collected while varying the attenuation with the results shown in Figure 3B. The transmission is a nonlinear curve indicative of saturable absorption which has the standard model:

$$T(I) = 1 - \frac{\alpha_s}{1 + I/I_{sat}} - \alpha_{ns}$$

where α_s is the modulation depth, I represents the power of the input light, I_{sat} is the saturable power, and α_{ns} is the nonsaturated loss. As shown in Figure 3B, the modulation depth is 23.7% at 1 μm, I_{sat} is 1.46 mW. This strong saturable absorption indicates that a V_2CT_x SA could be used as an ultrafast optical switch for ultrashort pulse generation.

4 Results and discussion

The schematic diagram of the mode-locked fiber laser based on hybrid SA is shown in Figure 4. A piece of 1.2 m Ytterbium (Yb)-doped fiber is forward pumped by a 980 pump via a 980/1064 wavelength division multiplexer. Two quarter-wave plates (QWP), a half-wave plate (HWP), and a polarizing beam splitter serve as a fast SA. The polarization adjusted by the HWP is used to maximize the diffraction efficiency of the diffraction grating. A 600 lines/mm grating with a collimator serves as a 4 nm BW Gaussian spectral filter. The fiber tapered V_2CT_x is spliced to the laser cavity. The total cavity length is ~4.5 m, which corresponds to the total dispersion 0.1 ps^2. The performance of the mode-locked fiber laser was measured by an optical spectrum analyzer (Yokogawa AQ6370D), an autocorrelator (APE pulseCheck), an oscilloscope

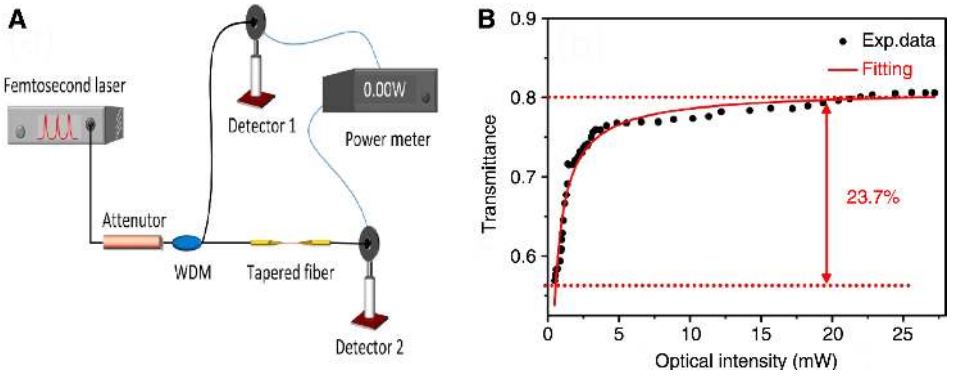

Figure 3: Nonlinear optical measurement of V_2CT_x.
(A) Nonlinear transmittance detector system. (B) Nonlinear transmission of V_2CT_x at 1 μm.

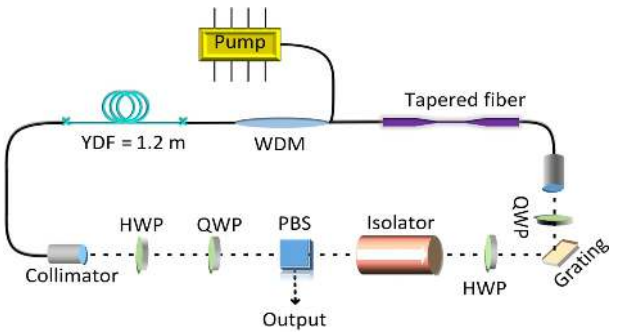

Figure 4: Experimental set up.

(Keysight DSOS104 A), and a radio-frequency (RF) analyzer (Keysight N9010B) with a high-speed photodetector.

To demonstrate the advantage of hybrid mode-locked function, we first measure the output performance of laser system with NPE first, and then insert the tapered fiber with MXene SA into the cavity for comparison. The output performance of the Yb-doped PML fiber laser with only NPE is shown in Figure 5. The cavity reached mode-locked operation at a threshold pump power of 344 mW and an output power of 21.20 mW. It is rare to find the cavity mode-locked prior to waveplate adjustment. Figure 5A, B shows that 45 nm output spectrum and the intensity autocorrelation of a 74 fs dechirped pulse, respectively. The pulse train interval was 26 ns (Figure 5C). Radio frequency (RF) spectrum of the laser is shown in Figure 5D. The fundamental cavity repetition rate was 35.8 MHz and the electrical SNR can reach up to 58 dB with 100 Hz resolution.

The slow SA V_2CT_x was spliced into the cavity to measure the properties of a hybrid SA PML fiber laser. The cavity reached mode-locked operation at a pump threshold of 260 mW with 28 mW output power without touching the waveplates (Figure 6A). This proves self-starting with low mode-locked operation is possible by incorporating V_2CT_x into the laser cavity. Figure 6B compares the NPE only and the NPE with MXene both pumped at 344 mW with 21.2 and 38.5 mW output powers, respectively. Figure 6C indicates the SNR was 71 dB, which increased 13 dB compared with NPE solely. Figure 6D shows that the dechirped autocorrelation of the hybrid SA reaches 72 fs, which is the shortest pulse duration generated from hybrid or 2D mode-locked fiber lasers. Hence, we conclude that the hybrid mode-locking technique increases output power 17.3 mW while broadening the bandwidth 3 nm and increasing the SNR 13 dB compared with using only NPE SA. These results show that hybrid mode-locking offers improved cavity

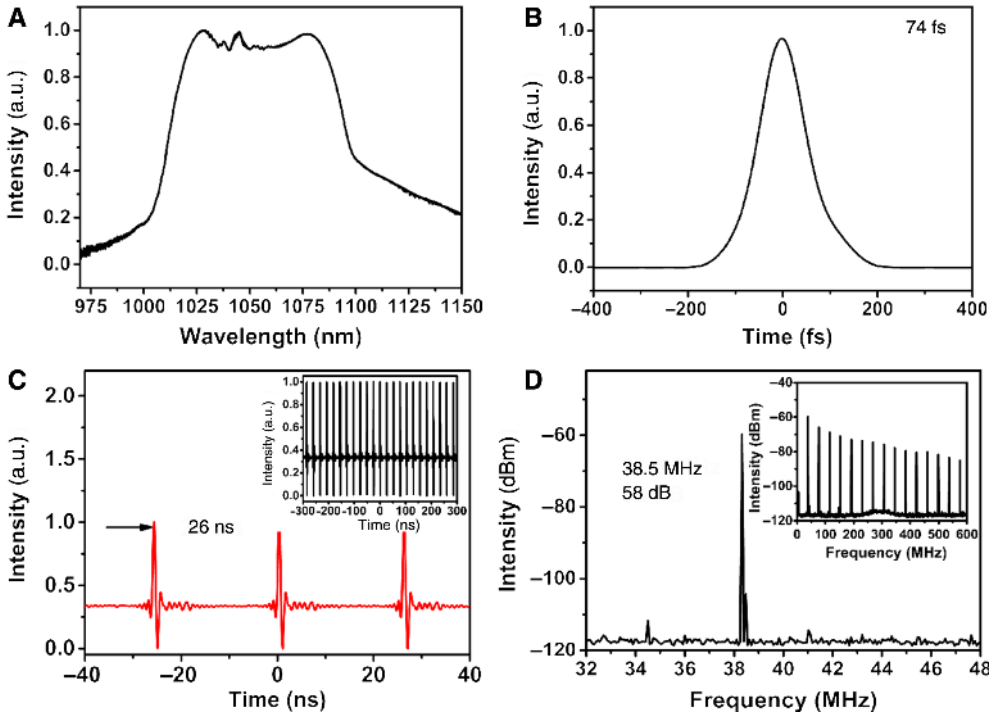

Figure 5: Laser output performance based on NPR saturable absorber solely.
(A) Output spectrum. (B) Dechirped autocorrelation. (C) Typical oscilloscope pulse trains of mode-locking, inset: broadband oscilloscope pulse trains. (D) Radio frequency (RF) spectrum of the mode-locked pulses, inset: broadband RF spectrum.

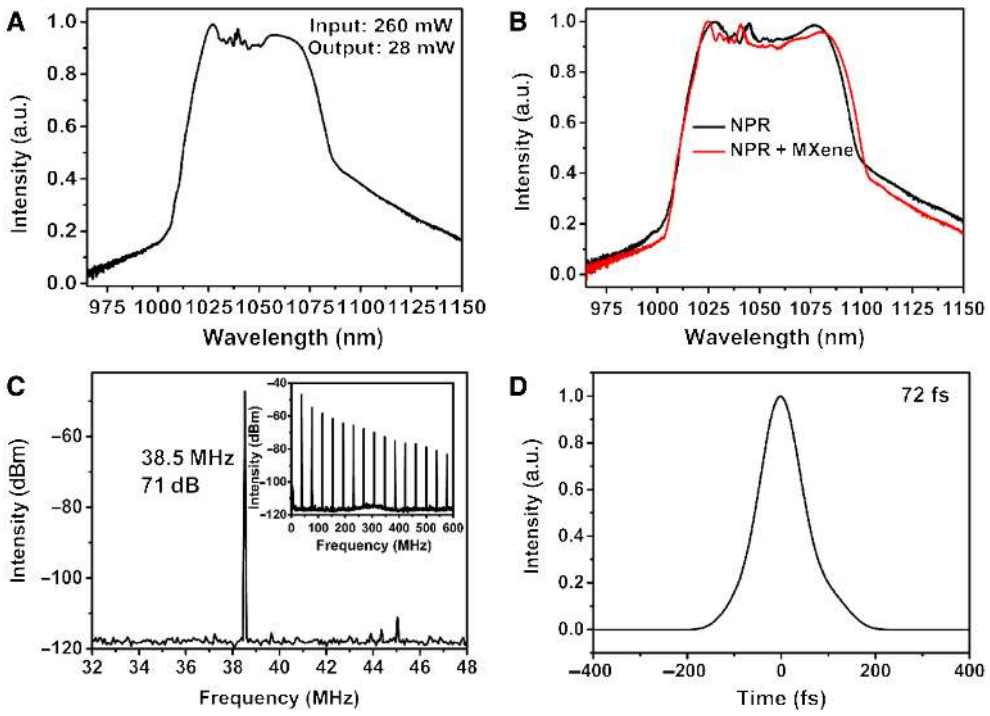

Figure 6: Output performance based on hybrid saturable absorber combines nonlinear polarization evolution (NPE) with V_2CT_x.
(A) Threshold spectrum. (B) Spectrum comparison at 344 mW pump power for NPE and NPE with MXene. (C) Radio frequency (RF) spectrum of the mode-locked pulses, inset: broadband RF spectrum. (D) Intensity autocorrelation of dechirped pulse.

efficiency and output pulse stability. Table 1 compares the output performance of the hybrid mode-locker with NPE only, highlighting the hybrid's improvement across all metrics.

Figure 7A shows that spectrum bandwidth and output power increase with pump power. Spectrum bandwidth and average power range from 45 to 62 nm and 28 to 60 mW, respectively. The pump power can reach upto 480 mW which indicates that MXene has a high damage threshold and is not destroyed by thermal accumulation. Figure 7B shows that the mode-locked operation can be maintained for 24 h without changing. It proved that hybrid mode-locking offers novel stability in output performance.

The article demonstrates a hybrid mode-locked Yb-doped fiber laser based on NPE and V_2CT_x that improves output performance across multiple metrics. First, the output spectrum became broader than using only NPE SA owing to the strong nonlinear effects of V_2CT_x, and the tapered fiber waist reduces the effective mode area to intentionally enhanced nonlinear effects. Second, the experiment results show that V_2CT_x has a high modulation depth (23.7%) and a high damage threshold, which exhibits potential advantages as a SA, especially for the ultra-short pulse generation with high energy. Next, the V_2CT_x SA achieves self-starting mode-locked operation and lowers mode-locked power threshold. At the same time the output power is nearly two times that of the NPE only laser at the same input power, demonstrating that hybrid mode-locking can reduce polarization loss. Finally, SNR can be increased 13 dB over NPE only, and the system can work 24 h continuously without changing, which proves that the hybrid mode-locked system is ultra-stable in the environment.

Table 1: Performance summary of Yb-doped mode-locked fiber lasers using saturable absorber separately.

	Output power (mW)	Pulse energy (nJ)	Bandwidth (nm)	Pulse duration (fs)	Signal to noise ratio (dB)
MXene	18	0.468	3	2300	71
NPE	21.20	0.55	45	74	58
Hybrid (NPR + Mxene)	38.5	1	48	72	71

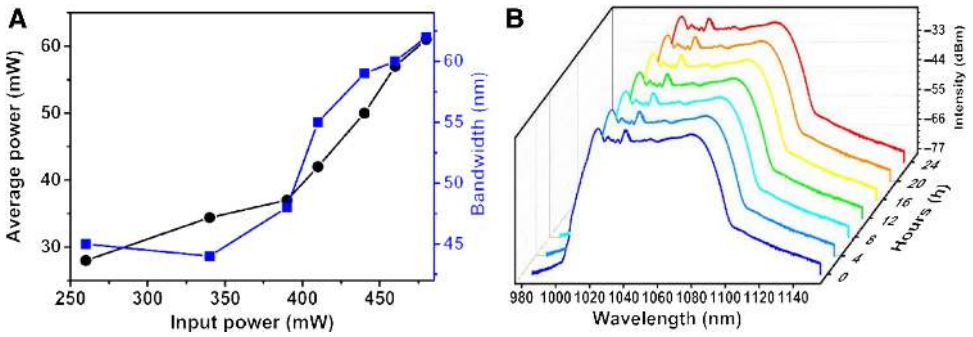

Figure 7: Output performance based on hybrid saturable absorber combines nonlinear polarization evolution (NPE) with V_2CT_x. (A) Output power and bandwidth with increase the pump power. (B) Spectrum by increasing hours.

5 Conclusion

In this article, V_2CT_x nanosheets were successfully fabricated and employed as an SA by directly depositing them on a tapered fiber. We investigate the advantages of MXene (V_2CT_x) for hybrid mode-locked fiber laser at 1 μm. Seventy-two fs pulses can be easily generated from a Yb-doped mode-locked fiber laser through the hybrid SA effect of V_2CT_x and NPE. This is the shortest pulse duration obtained from a hybrid mode-locked fiber laser or as well as a 2D material mode-locked laser system. Compared with using NPE only, V_2CT_x with NPE achieves self-starting mode-locked operation and a SNR increase of 13 dB. This proves that V_2CT_x will be a suitable SA for generating stable self-starting ultra-short pulses with high energy which will be beneficial for novel applications in areas such as nonlinear imaging and nanofabrication. Additionally, this self-starting mechanism may have potential for commercializing compact fiber laser systems with low maintenance and high performance.

Acknowledgments: C. M. and W. H. contributed equally to this work. The research was supported by the National Natural Science Foundation of China (Grant Nos. 61805147, Funder Id: http://dx.doi.org/10.13039/501100001809), the Science and Technique Planning Project of Guangdong Province (Grant No. 2016B050501005), and the Science and Technology Innovation Commission of Shenzhen (Grant No. JCYJ20180305125141661, and KQTD2015032416270385).

References

[1] Soong HK, Malta JB. Femtosecond lasers in ophthalmology. Am J Ophthalmol 2009;147:189–97.
[2] Macklin JJ, Kmetec JD, Gordon CL. High-order harmonic generation using intense femtosecond pulses. Phys Rev Lett 1993;70:766.
[3] Fermann ME, Hartl I. Ultrafast fibre lasers. Nat Photonics 2013;7:868–74.
[4] Xu C, Wise FW. Recent advances in fibre lasers for nonlinear microscopy. Nat Photonics 2013;7:875–82.
[5] Telle HR, Steinmeyer G, Dunlop AE, et al. Carrier-envelope offset phase control: a novel concept for absolute optical frequency measurement and ultrashort pulse generation. Appl Phys B 1999;69:327–32.
[6] Udem T, Reichert J, Holzwarth R, Hänsch TW. Absolute optical frequency measurement of the cesium D1 line with a mode-locked laser. Phys Rev Lett 1999;82:3568.
[7] Sugioka K, Cheng Y. Femtosecond laser three-dimensional micro- and nanofabrication. Appl Phys Rev 2014;1:041303.
[8] Chong A, Renninger WH, Wise FW. All-normal-dispersion femtosecond fiber laser with pulse energy above 20 nJ. Opt Lett 2007;32:2408.
[9] Grelu P, Akhmediev N. Dissipative solitons for mode-locked lasers. Nat Photonics 2012;6:84–92.
[10] Renninger WH, Chong A, Wise FW. Self-similar pulse evolution in an all-normal-dispersion laser. Phys Rev A 2010;82:021815.
[11] Ma C, Khanolkar A, Chong A. High-performance tunable, self-similar fiber laser. Opt lett 2019;44:1234–6.
[12] Oktem B, Ülgüdür C, Ilday FÖ. Soliton–similariton fibre laser. Nat Photonics 2010;4:307–11.
[13] Nelson LE, Jones DJ, Tamura K, Haus HA. Ultrashort-pulse fiber ring lasers. Appl Phys B 1997;65:277–94.
[14] Kurtner FX, der Au JA, Keller U. Mode-locking with slow and fast saturable absorbers-what's the difference? IEEE J Sel Top Quant 1998;4:159–68.
[15] Chen JC, Haus HA, Ippen EP. Stability of lasers mode locked by two saturable absorbers. IEEE J Sel Top Quant 1993;29:1228–32.
[16] Guina M, Xiang N, Vainionpää A, et al. Self-starting stretched-pulse fiber laser mode locked and stabilized with slow and fast semiconductor saturable absorbers. Opt Lett 2001;26:1809–11.
[17] Wang Y, Zhang F, Tang X, et al. All-optical phosphorene phase modulator with enhanced stability under ambient conditions. Laser Photonics Rev 2018;12:1800016.
[18] Song Y, Chen Y, Jiang X, et al. Nonlinear few-layer MXene-assisted all-optical wavelength conversion at telecommunication band. Adv Opt Mater 2019;7:1801777.
[19] Zhang H, Lu SB, Zheng J, et al. Molybdenum disulfide (MoS_2) as a broadband saturable absorber for ultra-fast photonics. Opt Express 2014;22:7249–60.
[20] Xia F, Wang H, Xiao D, et al. Two-dimensional material nanophotonics. Nat Photonics 2014;8:899–907.

[21] Chen H, Yin J, Yang J, et al. Transition-metal dichalcogenides heterostructure saturable absorbers for ultrafast photonics. Opt Lett 2017;42:4279–82.
[22] Zhang M, Wu Q, Zhang F, et al. Black-phosphorous-based pulsed lasers: 2D black phosphorus saturable absorbers for ultrafast photonics. Adv Opt Mater 2019;7:1970001.
[23] Kowalczyk M, Bogusławski J, Zybała R, et al. Sb_2Te_3-deposited D-shaped fiber as a saturable absorber for mode-locked Yb-doped fiber lasers. Opt Mater Express 2016;6:2273.
[24] Hasan T, Sun Z, Wang F, et al. Nanotube-polymer composites for ultrafast photonics. Adv Mater 2009;21:3874–99.
[25] Bao Q, Zhang H, Wang Y, et al. Atomic-layer graphene as a saturable absorber for ultrafast pulsed lasers. Adv Funct Mater 2009;19:3077–83.
[26] Guo Z, Zhang H, Lu S, et al. From black phosphorus to phosphorene: basic solvent exfoliation, evolution of raman scattering, and applications to ultrafast photonics. Adv Funct Mater 2015;25:6996–7002.
[27] Lu L, Wang W, Wu L, et al. All-optical switching of two continuous waves in few layer bismuthene based on spatial cross-phase modulation. ACS Photonics 2017;4: 2852–61.
[28] Zhou Q, Chen Q, Tong Y, Wang J. Light-induced ambient degradation of few-layer black phosphorus: mechanism and protection. Angew Chem Int Ed 2016;55:11437–41.
[29] Xing C, Huang W, Xie Z, et al. Ultrasmall bismuth quantum dots: facile liquid-phase exfoliation, characterization, and application in high-performance UV-Vis photodetector. ACS Photonics 2018;5:621–9.
[30] Buscema M, Groenendijk DJ, Blanter SI, et al. Fast and broadband photoresponse of few-layer black phosphorus field-effect transistors. Nano Lett 2014;14:3347–52.
[31] Anasori B, Lukatskaya MR, Gogotsi Y. 2D metal carbides and nitrides (MXenes) for energy storage. Nat Rev Mater 2017;2:16098.
[32] Mashtalir O, Naguib M, Mochalin VN, et al. Intercalation and delamination of layered carbides and carbonitrides. Nat Commun 2013;4:1716.
[33] Shahzad F, Alhabeb M, Hatter CB, et al. Electromagnetic interference shielding with 2D transition metal carbides (MXenes). Science 2016;353:1137–40.
[34] Zhao C, Wang Q, Zhang H, et al. Two-dimensional titanium carbide/RGO composite for high-performance supercapacitors. ACS Appl Mater Interfaces 2016;8:15661–7.
[35] Zhang CJ, Pinilla S, McEvoy N, et al. Oxidation stability of colloidal two-dimensional titanium carbides (MXenes). Chem Mater 2017;29:4848–56.
[36] Liu F, Liu Y, Zhao X, et al. Prelithiated V_2C MXene: a high-performance electrode for hybrid magnesium/lithium-ion batteries by ion cointercalation. Small 2020;16:1906076.
[37] Huang D, Xie Y, Lu D, et al. Demonstration of a white laser with V_2C MXene-based quantum dots. Adv Mater 2019;31:1901117.
[38] Vahid Mohammadi A, Mojtabavi M, Caffrey NM, et al. Assembling 2D MXenes into highly stable pseudocapacitive electrodes with high power and energy densities. Adv Mater 2019;31:1806931.

Supplementary Material: The online version of this article offers supplementary material (https://doi.org/10.1515/nanoph-2019-0527).